

## Identification of 3-(Acylamino)azepan-2-ones as Stable Broad-Spectrum Chemokine Inhibitors Resistant to Metabolism in Vivo

David J. Fox,<sup>\*,†</sup> Jill Reckless,<sup>‡</sup> Sibylle M. Wilbert,<sup>§,||</sup> Ian Greig,<sup>†</sup> Stuart Warren,<sup>†</sup> and David J. Grainger<sup>‡</sup>

Department of Chemistry, University of Cambridge, Lensfield Road, Cambridge, U.K., Department of Medicine, University of Cambridge, Box 157, Addenbrooke's Hospital, Cambridge CB2 2QQ, U.K., and NeoRx Corporation, 300 Elliot Avenue West, Suite 300, Seattle, Washington 98119

Received August 5, 2004

3-(Acylamino)glutarimides, a class of broad spectrum chemokine inhibitors, are rapidly hydrolyzed in serum, despite being stable in aqueous solution. Synthesis and high-performance liquid chromatography analysis of the proposed *N*-acyl-glutamate and -glutamine metabolites establish the enzyme-catalyzed breakdown pathways. In vitro assays suggest that despite their short half-life in vivo, the parent acylamino-glutarimides, not the ring-opened hydrolysis products, are the source of the antiinflammatory activity. Identification of this metabolic pathway has led to the development of 3-(acylamino)azepan-2-ones that are also broad spectrum chemokine inhibitors and act as stable, orally available powerful antiinflammatory agents in vivo with doses of 1 mg/kg.

### Introduction

Inflammation is an important component of both physiological host defense and pathological leukocyte recruitment. Increasingly, however, it is clear that temporally or spatially inappropriate inflammatory responses play a part in a wide range of diseases, not only in those with an obvious leukocyte component (autoimmune diseases, asthma, or atherosclerosis) but also in diseases that have not traditionally been considered to involve leukocytes such as osteoporosis or Alzheimer's disease.<sup>1–6</sup>

The chemokines are a large family of signaling molecules with homology to interleukin-8 that have been implicated in regulating leukocyte trafficking, both in physiological and in pathological conditions.<sup>7–11</sup> With more than 50 ligands and 20 receptors involved in chemokine signaling, the system has the requisite information density to address leukocytes through the complex immune regulatory processes from the bone marrow to the periphery then back through secondary lymphoid organs. However, this complexity of the chemokine system has hindered pharmacological approaches to modulating inflammatory responses through chemokine receptor blockade. It has proved difficult to determine which chemokine receptor(s) should be inhibited to produce therapeutic benefit in a given inflammatory disease.

More recently, a family of agents which simultaneously block signaling by a wide range of chemokines has been described. The first such agent, a peptide termed peptide 3, was found to inhibit leukocyte migration induced by five different chemokines, while leaving migration in response to other chemoattractants such

as formyl-methionyl-leucyl-proline peptide (fMLP) or transforming growth factor type- $\beta$  (TGF- $\beta$ ) unaltered.<sup>12</sup> This peptide and its analogues such as NR58-3.14.3,<sup>13</sup> collectively termed broad-spectrum chemokine inhibitors (BSCIs),<sup>14</sup> have subsequently been shown to have potentially useful antiinflammatory activity in a range of animal models of disease.<sup>13–15</sup> Interestingly, simultaneous blockade of multiple chemokines is not apparently associated with acute or chronic toxicity, suggesting this approach may be a useful strategy for developing new antiinflammatory medications with similar benefits to steroids but with reduced side effects.

However, peptides and peptoid derivatives such as NR58-3.14.3 may not be optimal for use in vivo. They are expensive to synthesize and have relatively unfavorable pharmacokinetic and pharmacodynamic properties. For example, NR58-3.14.3 is not orally bioavailable and is cleared from blood plasma with a  $t_{1/2}$  of less than 30 min after intravenous injection.<sup>16</sup> After an extensive structure/function analysis of the peptide 3 molecule, we identified the critical motif as WXQ (where W represents tryptophan, Q represents glutamine, and X represents any proteogenic amino acid). We went on to synthesize a number of non-peptide WXQ analogues and demonstrated that substituted acylamino-glutarimides retained the broad spectrum chemokine inhibitory activity of the parental peptide sequences, active in the low nanomolar concentration range.<sup>17</sup> The best of this series of compounds, (*S*)-3-(10'-undecenoylamino)glutarimide (**1**, NR58,4), inhibited chemokine-induced leukocyte migration with an ED<sub>50</sub> value of 5 nM and blocked the acute inflammatory responses to bacterial lipopolysaccharide at low doses in vivo (Figure 1).<sup>17</sup>

More recently, however, it has become clear that, while imide **1** is an effective antiinflammatory agent in models of acute inflammation, it is much less effective than the parental peptides such as NR58-3.14.3 in models of chronic inflammation (data not shown). In the present study therefore, we have characterized the pharmacokinetics of acylamino-glutarimides and

\* Author to whom correspondence should be addressed. Phone: +44 1223 336361. Fax: +44 1223 336362. E-mail: djf34@cam.ac.uk.

<sup>†</sup> Department of Chemistry, University of Cambridge.

<sup>‡</sup> Department of Medicine, University of Cambridge.

<sup>§</sup> NeoRx Corporation.

<sup>||</sup> Present address: ZymoGenetics, Inc., 1201 Eastlake Avenue East, Seattle, WA 98102-3702.

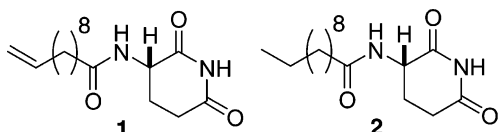
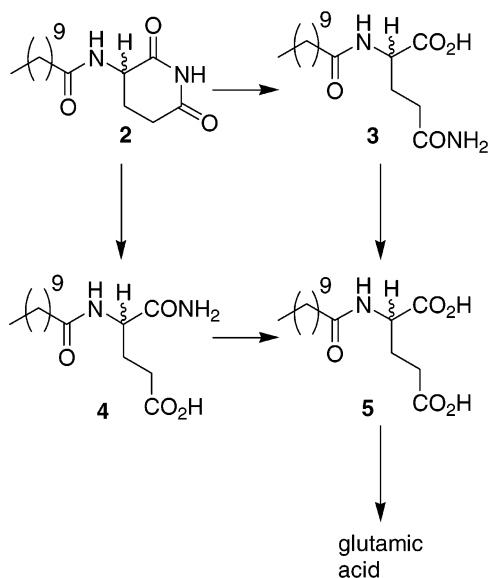


**Figure 1.** Small molecule broad-spectrum chemokine inhibitors.

**Scheme 1.** Possible Serum Catalyzed Hydrolysis Routes of Imide **2** in Vivo

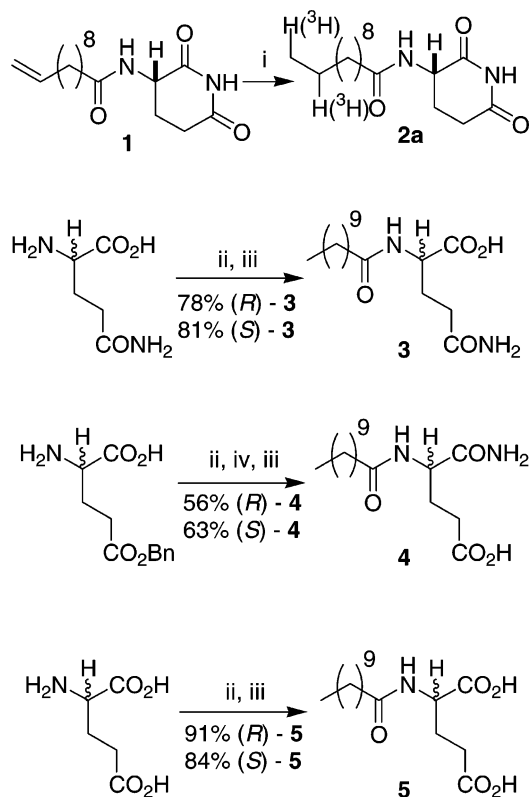


dissected their metabolic fate in vivo. These studies suggest that the lack of potency of these agents in models of chronic inflammation is due to the susceptibility of the aminoglutaramide ring to enzyme-catalyzed metabolism. We therefore synthesized and characterized a range of analogues of imide **1** (NR58,4) for retention of BSCI activity but increased metabolic stability. In this way, we identified a series of (acylamino)azepan-2-ones as potent BSCIs in vitro and antiinflammatory agents in vivo with excellent metabolic stability.

## Results and Discussion

To assess the pharmacokinetics of the acylamino-glutarimides, we synthesized a tritiated analogue of imide **1** by reacting the unsaturated parent compound with tritium gas over a palladium catalyst (Scheme 2). The resulting saturated compound (*S*)-3-(undecanoylamino)glutarimide (**2a**) had a specific activity of 50 Ci/mmol and comparable bioactivity to the parent imide **1** as an inhibitor of macrophage chemoattractant protein-1 (MCP-1)-induced migration of THP-1 cells, assayed exactly as described previously.<sup>12</sup> The specific activity was subsequently adjusted as required by addition of unlabeled imide **2**. [<sup>3</sup>H]-imide **2a** (100 μg, 0.33 μmol, 15 μCi) was injected intravenously into groups of three rats, and blood samples were taken at various times after injection. After preparation of serum from the blood samples, the total tritium content was determined as well as the fraction of the tritium present in the unchanged drug measured by high-performance liquid chromatography (HPLC). Total tritium decreased in the blood very slowly, with a half-time of approximately 56 h, but by 48 h none of the tritium was present in the form of the injected drug. This suggested that imide **2**

**Scheme 2.** Reagents: (i) <sup>1</sup>H<sub>2</sub>(<sup>3</sup>H<sub>2</sub>), Pd/C; (ii) 10-undecenoyl chloride, Na<sub>2</sub>CO<sub>3</sub>, H<sub>2</sub>O, CH<sub>2</sub>Cl<sub>2</sub>; (iii) H<sub>2</sub>, Pd(OH)<sub>2</sub>/C, THF; (iv) DCC, NHS, THF then NH<sub>3</sub> (aq)



was undergoing rapid metabolism to yield stable metabolites that were only slowly excreted (Figure 2).

To investigate the nature of this metabolism further, imide **2** (10 μM) was incubated in saline, urine, and serum at various temperatures, and the amount of intact drug was assayed by reverse-phase HPLC. More than 90% of the imide **2** remained intact after 7 days in saline solution or in urine at both 4 and 37 °C, suggesting the molecule was intrinsically very stable in aqueous solution. In contrast, there was considerable degradation of the drug in serum at 37 °C with less than 20% of the drug intact after 6 h (Figure 3). The substantially lower rate of degradation in serum at 4 °C and room temperature, together with the stability in saline, suggested that this degradation might be enzymatic. To test this hypothesis, imide **2** was incubated in heat-denatured serum at 37 °C for various periods. Degradation was substantially slower than that observed in native serum, with 50% of the drug still intact after 8 h.

During incubation in native serum at 37 °C, the single peak corresponding to intact imide **2** was gradually replaced first by two peaks with very similar retention time and then by a single peak that eluted significantly earlier (Figure 4). Such a pattern of degradation is consistent with hydrolytic ring opening of the glutarimide to both the *N*α-substituted glutamine (**3**) and the -isoglutamine (**4**) metabolites. Both primary amides are then hydrolyzed to yield *N*-substituted glutamic acid. To test this hypothesis, the metabolites **3**, **4**, and **5** were synthesized and subjected to reverse-phase HPLC. The retention times of *N*α-undecanoyl glutamine and *N*α-undecanoyl isoglutamine matched the retention times of the two peaks representing the primary metabolites

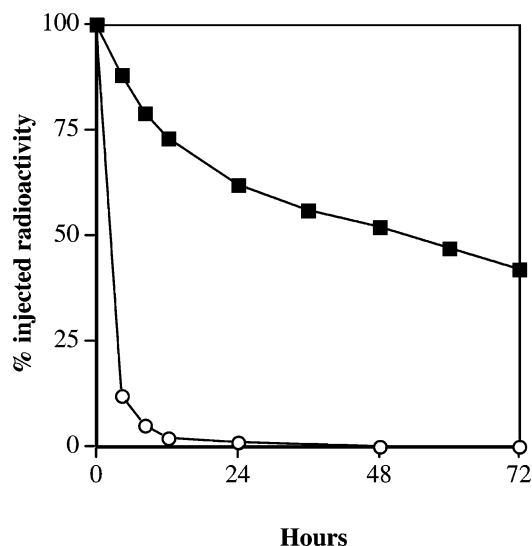


**Figure 2.** Pharmacokinetics of [ $^3\text{H}$ ]-imide **2a** after iv administration.  $0.33 \mu\text{mol}$  ( $15 \mu\text{Ci}$ ) of [ $^3\text{H}$ ]-imide **2a** was injected intravenously via the tail vein into adult (250–300 g) male Wistar rats at time 0. Blood samples were taken at various times after injection and split into two. Half was processed for total radioactive counts, expressed as a percentage of the injected dose (closed squares), and half was subjected to HPLC analysis, expressing the counts present in the peak representing NR58,26 **2** as a percentage of the injected dose (open circles). Data are from a single rat and representative of three identical studies.

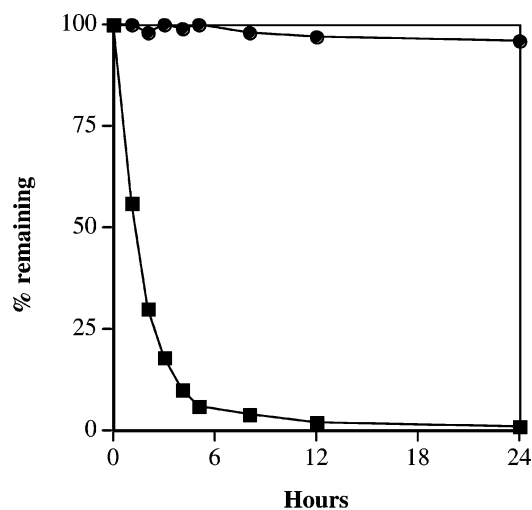


**Figure 3.** Degradation of imide **2** in vitro. Unlabeled imide **2** was incubated ( $10 \mu\text{M}$ ) in phosphate-buffered saline pH 7.4 (circles) or human serum (squares) at  $37^\circ\text{C}$ . At various time points, samples were removed and analyzed by reverse-phase HPLC. The percentage of compound remaining was expressed as the peak area at each time point as a percentage of the peak area at time 0.

of imide **2** in serum. Furthermore, spiking them into the mixture of degradation products resulted in no additional peaks in the chromatogram. Similar findings were obtained using *N*-undecanoyl glutamic acid, confirming the degradation pathway of imide **2** as suggested in Scheme 1.

Another potential route of degradation that would not be identified by these HPLC experiments is racemization. Imide (*R*)-**1** was synthesized in racemization-free conditions from (*R*)-glutamine, as for its *S* enantiomer.<sup>17</sup> The *R* enantiomer is at least 50-fold less active than its

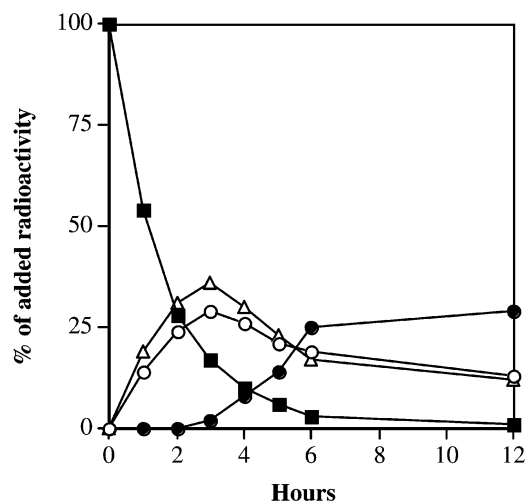


**Figure 4.** Degradation of imide **2** in vitro. The time course of accumulation of three major metabolites of imide **2** in human serum at  $37^\circ\text{C}$  is shown. *N*-Acyl-glutamine (**3**, open circles) and *N*-acyl-isoglutamine (**4**, open triangles) accumulate first, followed by *N*-acyl-glutamate (**5**, filled circles). The degradation of the starting material is shown for comparison (filled squares). The identity of the metabolites was established by spiking in various chemically synthesized putative metabolite prior to chromatographic analysis.

**Table 1.** In Vitro BSCI Activity of Acylamino-Glutarimides and Metabolites

metabolite	ED <sub>50</sub> /nM	metabolite	ED <sub>50</sub> /nM
( <i>S</i> )- <b>1</b>	5	( <i>S</i> )- <b>4</b>	15 000
( <i>R</i> )- <b>1</b>	250	( <i>R</i> )- <b>4</b>	40 000
( <i>S</i> )- <b>2</b>	10	( <i>S</i> )- <b>5</b>	10 000
( <i>R</i> )- <b>2</b>	not tested	( <i>R</i> )- <b>5</b>	25 000
( <i>S</i> )- <b>3</b>	30 000	( <i>S</i> )-glutamic acid	>100 000
( <i>R</i> )- <b>3</b>	50 000	( <i>R</i> )-glutamic acid	>100 000

*S* enantiomer in an in vitro leukocyte migration assay (Table 1). Consequently, any racemization occurring in vivo would reduce the activity of the drug. To assess the rate of racemization in aqueous medium, we synthesized a model compound (*S*)-3-(pentanoylamino)-glutarimide,<sup>17</sup> which is sufficiently soluble in buffered saline D<sub>2</sub>O at pH 7, to allow measurement of deuterium exchange at the stereocenter by NMR spectroscopy. These studies demonstrated that deuterium incorporation did not occur to any measurable extent after 24 h at  $37^\circ\text{C}$ . Racemization therefore does not occur at any significant rate in these conditions. However, it remains possible that acylamino-glutarimides undergo protein-catalyzed racemization in serum as shown for thalidomide,<sup>18,19</sup> and on the basis of results presented here we cannot definitively exclude a similarly catalyzed contribution to the racemization of imide **1** (NR 58,4) in vivo.

We conclude that imide **1** (NR58,4) and related acylamino-glutarimides undergo rapid degradation in vivo as a result of enzymatic ring opening of the glutarimide ring. The resulting *N* $\alpha$ -acyl-glutamine (**3**) and isoglutamine (**4**) metabolites then hydrolyze more slowly to yield *N*-acyl glutamic acid (**5**). Any further metabolism, such as cleavage of the amide linker between the acyl side chain and the aminoglutaramide head structure, does not occur at any appreciable rate in comparison to the ring-opening reaction described here. However, a tritium-containing peak corresponding

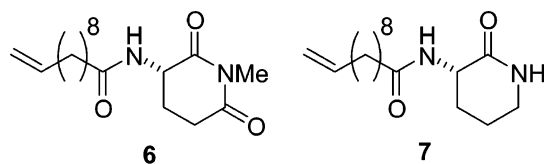


**Figure 5.** BSCIs more stable than imide **1**.

to *N*-undecanoyl-glutamate (**5**) was absent from serum 48 h after a single injection of [<sup>3</sup>H]-imide **2** in vivo.

Next, we tested whether the metabolites of imide **2** might possess any biological activity in the chemokine-induced leukocyte migration assay. Both *R* and *S* enantiomers of *N*α-undecanoyl glutamine (**3**), *N*α-undecanoyl-isoglutamine (**4**), and *N*-undecanoyl-glutamic acid (**5**) as well as (*R*)- and (*S*)-glutamate, were tested for broad-spectrum chemokine inhibitory activity as previously described.<sup>12</sup> The BSCI activity of parental imide **1** (NR58,4), imide **2**, and its metabolites are shown in Table 1. All metabolites tested are significantly less active than **2**. It is likely that the rapid degradation of the core aminoglutaramide ring to yield biologically inactive metabolites is responsible for the striking difference in activity between imide **1** and the stable peptide structures such as NR58-3.14.3 when compared in models of chronic inflammation.

Imide **1** (NR58,4) therefore represents a model for non-peptide broad-spectrum chemokine inhibitors (BSCIs), having comparable activity to the parental peptide structures such as NR58-3.14.3 in leukocyte migration assays in vitro and in models of acute inflammation in vivo. However, the utility of such acylamino-glutarimides as antiinflammatory drugs is likely to be severely curtailed by the rapid metabolism and consequent inactivation described here. Any possibility of using these non-peptide BSCIs in vivo depends on the identification of structures that retain the biological activity of the acylamino-glutarimides but that are resistant to enzyme-catalyzed degradation to inactive metabolites.

Our previous studies identified at least two analogues of (*S*)-3-(undec-10'-enoyl)aminoglutaramide (**1**, NR58,4) with modifications to the aminoglutaramide ring that retained BSCI activity, albeit with a considerable loss of potency compared with the parental structure. (*S*)-3-(Undec-10-enoylamino)-1-methyl-glutarimide (**6**) inhibits MCP-1-induced leukocyte migration with an ED<sub>50</sub> value of 33 nM, while the related six-membered lactam **7** has an ED<sub>50</sub> value of 100 nM in the same assay (Figure 5).<sup>17</sup> We therefore tested the stability of *N*-methyl-imide **6** and lactam **7** in saline and serum at 37 °C. In comparison to imide **1** (NR58,4), lactam **7** was considerably more stable, with less than 10% of the compound undergoing metabolism in 24 h, consistent with expected increased stability of the lactam ring compared with the imide. In contrast, although the *N*-methyl-imide **6** was metabolized slightly slower than the parental compound, it was still rapidly degraded in serum at 37 °C, presumably via the same enzymatic ring-opening mechanism as imide **1**.

Lactam **7** therefore represents an analogue of imide **1** with BSCI activity that is resistant to degradation in serum. Thus, we synthesized further analogues of this structure in an attempt to identify new compounds that retained the stability of six-membered ring lactam **7** but

**Table 2.** In Vitro Activity of (*R*)- and (*S*)-3-(Acylamino)lactams **7–17**

	( <i>S</i> )- <b>7</b> ED <sub>50</sub> = 100 nM
	( <i>S</i> )- <b>8</b> ED <sub>50</sub> = 245 nM
	( <i>S</i> )- <b>9</b> ED <sub>50</sub> = 40 nM
	( <i>S</i> )- <b>11</b> ED <sub>50</sub> = 10 nM
	n=9 ( <i>S</i> )- <b>10</b> ED <sub>50</sub> = 50 nM
	n=10 ( <i>S</i> )- <b>12</b> ED <sub>50</sub> = 15 nM
	n=12 ( <i>S</i> )- <b>13</b> ED <sub>50</sub> = 5 nM
	n=14 ( <i>S</i> )- <b>14</b> ED <sub>50</sub> = 3 nM
	n=14 ( <i>R</i> )- <b>14</b> ED <sub>50</sub> = 40 nM
	n=16 ( <i>S</i> )- <b>15</b> not tested
	( <i>S</i> )- <b>16</b> ED <sub>50</sub> = 3 nM
	( <i>S</i> )- <b>17</b> ED <sub>50</sub> = 3 nM
	( <i>R</i> )- <b>17</b> ED <sub>50</sub> = 30 nM

have increased potency. Initially, we synthesized the related five- and seven-membered ring lactam compounds (**8** and **9**). The seven-membered ring lactam (**9**) was somewhat more active than the six-membered and five-membered ring compounds, displaying an increase in activity with increasing ring size (Table 2), inhibiting MCP-1-induced leukocyte migration<sup>12</sup> with an ED<sub>50</sub> value of 40 nM.

However, seven-membered ring lactam **9** was still almost 10-fold less potent in vitro than NR58,4 (**1**). In the series of acylamino-glutarimide compounds,<sup>17</sup> imide **1** is more potent than its terminally saturated analogue imide **2**. Synthesis of the saturated caprolactam **10** and terminal alkyne version **11** showed that there is again a slight trend of increasing potency with decreasing saturation at the side chain terminus (Table 2). In our previous study, we had shown that there was a trend to increasing potency of the *N*-acylamino-glutarimides as the acyl chain lengthened, although this effect seemed to be maximal with a chain length longer than eight carbons. We therefore tested whether lengthening

the acyl side chain still further might increase the potency of the 3-(acylamino)azepan-2-one series based on compound **10**. Consequently, we synthesized C<sub>12</sub>, C<sub>14</sub>, C<sub>16</sub>, and C<sub>18</sub> side chain analogues (**12–15**). In contrast to the aminoglutarimide series published previously, we found that increasing chain length was associated with further increase in potency right up to a C<sub>16</sub> side chain (lactam **14**). The saturated C<sub>18</sub> side chain is insufficiently soluble even in dimethyl sulfoxide (DMSO) to allow its biological activity in an aqueous system to be tested (Supporting Information). Synthesis of (*S*)-3-(hexadecanoylamino)azepan-2-one (**14**) has reclaimed the activity of imide **1** (NR58,4) but with superior stability.

Among the 3-(acylamino)glutarimides, we had previously found that the *S* enantiomers were considerably more active than the *R* enantiomers (between 15- and 30-fold more active, depending on the acyl chain under study). We therefore compared the activity of (*S*)-3-(hexadecanoylamino)azepan-2-one (**14**) with its *R* enantiomer in the bioassay. Consistent with our previous data, we found the *S* enantiomer (ED<sub>50</sub> = 3 nM) was considerably more active than the *R* enantiomer (ED<sub>50</sub> = 40 nM).

Finally, we examined the stability of lactam (*S*)-**14** in serum. The drug (10 μM) was incubated in saline solution or in serum at 4 °C, room temperature, and 37 °C, and the metabolism of the drug was followed by reverse-phase HPLC. Consistent with the stability of the six-membered ring lactam **7**, we found that <10% of the lactam (*S*)-**14** had been degraded after 24 h, even in serum at 37 °C. We conclude that lactam (*S*)-**14** represents a stable and potent non-peptide BSCI with considerable potential for development as an anti-inflammatory therapy in vivo.

Unfortunately, lactam (*S*)-**14** is not soluble enough in the aqueous DMSO solvent required for in vivo study. To maintain the biological activity and improve the solubility of the compounds, unsaturated versions of the C<sub>16</sub> and C<sub>18</sub> side chain compounds were synthesized from palmitoleic and oleic acid, respectively. The (*S*)-3-(acylamino)azepan-2-ones (*S*)-**16** and (*S*)-**17** have the same in vitro activity as the saturated C<sub>16</sub> compound lactam (*S*)-**14** (3 nM) but are indeed more soluble (Supporting Information). The *R* enantiomer of the oleoyl compound (**17**) is less active (30 nM) in the in vitro assay as with the *R* enantiomers of 3-(10'-undecenoylamino)glutarimide (**1**, NR58,4) and 3-(hexadecanoylamino)azepan-2-one (**14**).

Lactams (*S*)-**16** and (*S*)-**17** (BN 83253) represent a considerable improvement in properties compared with NR58,4. They have similar potency as a BSCI in vitro but are relatively resistant to metabolism in serum. Unlike the saturated long-chain lactams (such as **15**), these compounds are also sufficiently soluble in DMSO-containing vehicles to allow their antiinflammatory properties in vivo to be determined. We therefore tested lactams (*S*)-**16** and (*S*)-**17** in the sublethal lipopolysaccharide (LPS)-induced endotoxemia mouse model that we have used previously as a rapid assay of antiinflammatory potential.<sup>17</sup> A single subcutaneous injection of lactams (*S*)-**16** or (*S*)-**17** was administered 30 min prior to intraperitoneal injection of 750 μg of bacterial LPS. Two hours later, the extent of the

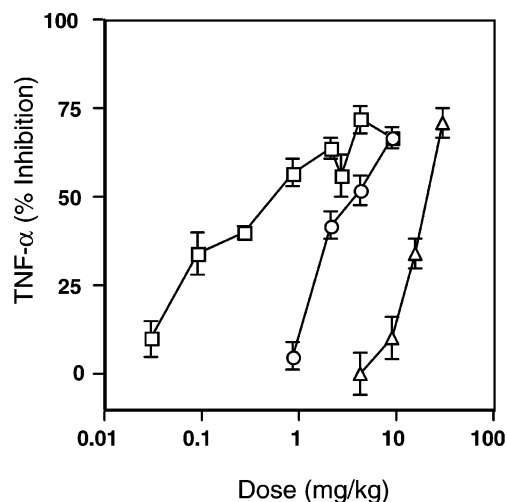


**Figure 6.** In vivo activity of acylamino-lactams: (*S*)-**16** (subcutaneous dose as open circles), (*S*)-**17** (subcutaneous dose as open squares), and cyclic peptide NR58-3.14.3 (subcutaneous dose as open triangles).

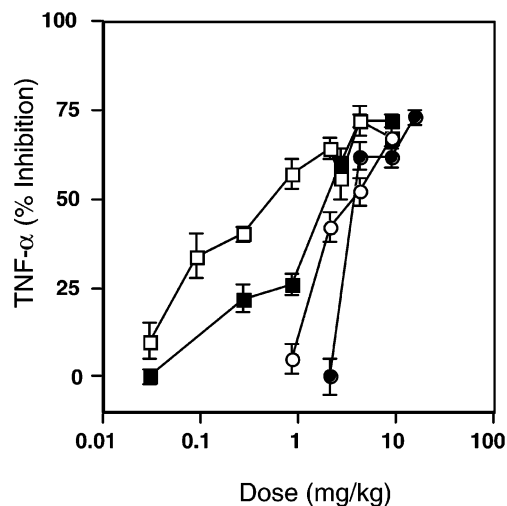
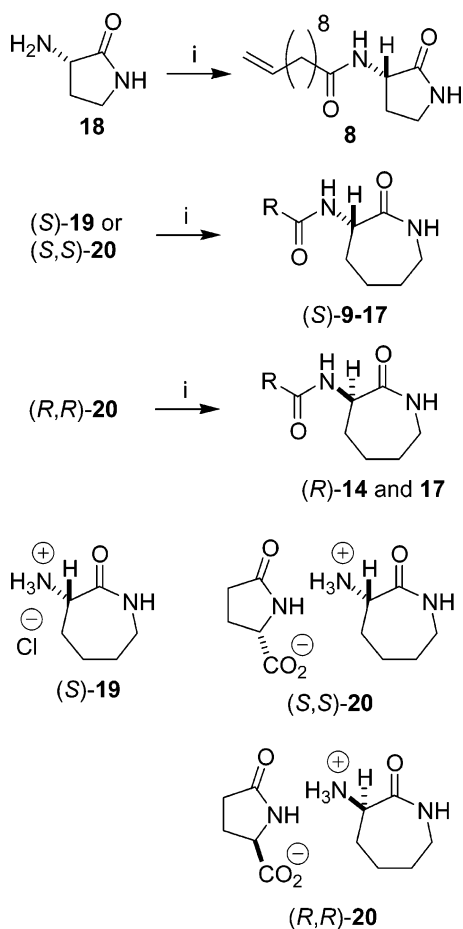


**Figure 7.** In vivo activity of acylamino-lactams: (*S*)-**16** (subcutaneous dose as open circles, oral dose as filled circles) and (*S*)-**17** (subcutaneous dose as open squares, oral dose as filled squares).

systemic inflammatory response was estimated by measuring the level of the proinflammatory cytokine TNF-α in serum (Figure 6). Both lactams (*S*)-**16** and (*S*)-**17** suppressed the LPS-induced increase in serum TNF-α in a dose-dependent fashion, with a maximal reduction of 60–70%, exactly as seen previously with NR58,4 and thalidomide.<sup>17</sup> Lactam (*S*)-**17** was more potent than lactam (*S*)-**16** with an ED<sub>50</sub> for suppression of TNF-α (with respect to the maximal effect) of 0.1 mg/kg.

Neither NR58-3.14.3 nor the acylamino-glutarimides (such as NR58,4) had appreciable oral bioavailability (<0.1% AUC versus intravenous administration for NR58-3.14.3). We therefore tested whether the more stable (acylamino)azepin-2-ones, such as lactam (*S*)-**17**, might represent the first orally bioactive BSCI compounds. A single dose of lactam (*S*)-**17**, administered by oral gavage 45 min prior to intraperitoneal injection of LPS, suppressed LPS-induced TNF-α levels in serum in a dose dependent fashion, with a maximal suppression similar to that observed following subcutaneous administration of lactam (*S*)-**17**. However, the potency

**Scheme 3.** Reagents: (i) RCOCl, Na<sub>2</sub>CO<sub>3</sub>, H<sub>2</sub>O, CH<sub>2</sub>Cl<sub>2</sub>.



of the compound was significantly less following oral administration ( $ED_{50} = 1$  mg/kg with respect to the maximal effect). Although the compounds are obviously very lipophilic, they do show a degree of activity, albeit low, when administered orally. An accurate measure of the oral bioavailability, via comparison with intravenous administration, would have to be made to confirm the indirect observations obtained from the functional inflammatory assays.

BSCIs represent a promising new class of agents with antiinflammatory effects in vivo. The original peptides first identified as chemokine inhibitors were not ideal for administration in vivo, due in part to unsuitable pharmacokinetics. While acylamino-glutarimides were then shown to possess similar BSCI activity and anti-inflammatory effects in acute models of inflammation, here we show that these compounds are subject to enzyme-catalyzed metabolism, resulting in rapid conversion to inactive products. In contrast, the 3-(acylamino)azepan-2-ones described here retain BSCI activity comparable to the peptide NR58-3.14.3 and the acylamino-glutarimide NR58,4 but are relatively resistant to enzymatic metabolism. As a result, this series of acylamino-lactams, the most potent member being lactam (S)-17 (BN 83253), has powerful antiinflammatory properties in vivo that make the molecules attractive candidates for further development as antiinflammatory drugs.

**Synthesis.** Imide (R)-1 was synthesized according to the procedure for its enantiomer.<sup>17</sup> Glutamine and glutamic acid derivatives **3** and **5** were made by a simple

acylation/hydrogenation route from enantiomerically pure amino acids (Scheme 2). Isoglutamine derivative **4** was made in a similar way from glutamic acid  $\gamma$ -benzyl ester, but involving the conversion of the unprotected acid into an amide before deprotection. Acylamino-lactams were synthesized by acylation of the relevant amino-lactam; (S)-3-(10-undecenoylamino)pyrrolidin-2-one (**8**) was synthesized by acylation of (S)-3-amino-pyrrolidin-2-one<sup>20</sup> (**18**, Scheme 2). Enantiomerically pure salts of (S)-3-amino-azepan-2-one, with either chloride (S)-19 or pyroglutamate counterions (S,S)-20, were synthesized according to published methods,<sup>21,22</sup> and pure (R)-3-amino-azepan-2-one was isolated as its (R)-pyroglutamate salt (R,R)-20 in an analogous fashion. Acylation with a range of acid chlorides giving (S)-3-(acylamino)azepan-2-ones **9–17**, (R)-14, and (R)-17 was achieved using water/dichloromethane mixtures and sodium carbonate as a base (Scheme 3, Table 2).

## Experimental Section

**Synthesis.** Flash column chromatography was carried out using Merck Kieselgel 60 (230–400 mesh). Thin-layer chromatography was carried out on commercially available pre-coated plates (Merck Kieselgel 60F<sub>254</sub>). Proton and carbon NMR spectra were recorded on a Bruker Avance 500 Fourier transform spectrometer using an internal deuterium lock. Chemical shifts are quoted in parts per million downfield of tetramethylsilane, and values of coupling constants (*J*) are given in Hz. Carbon NMR spectra were recorded with broad band proton decoupling and distortionless enhancement by polarization transfer. Melting points were measured on a Stuart Scientific melting point apparatus (SMP 1) and are uncorrected. Infrared spectra were recorded on a Perkin-Elmer Spectrum One (FT-IR) spectrophotometer. Electrospray (ES) mass spectra were recorded using a Micromass Q-ToF instrument. Microanalyses were carried out by the staff of the University Chemical Laboratory using a CE440 elemental analyzer from Exeter Analytical, Inc. Optical rotations were recorded on a Perkin-Elmer 241 polarimeter (using the sodium D line, 589 nm). Specific rotations are given in units of 10<sup>-1</sup> deg dm<sup>2</sup> g<sup>-1</sup>. Acid chlorides were used as supplied or made by addition of one equivalent of oxalyl chloride to the relevant carboxylic acid and used without purification.

(R)-3-(10'-Undecenoylamino)glutarimide (**1**) was synthesized according to the method for the (S)-enantiomer,<sup>17</sup> from (R)-glutamine in 37% yield.

(S)-N $\alpha$ -(Undecanoyl)glutamine (**3**). (S)-Glutamine (2 mmol) and Na<sub>2</sub>CO<sub>3</sub> (6 mmol) in water (50 mL) were added to a solution of undec-10-enoyl chloride (2 mmol) in tetrahydrofuran (THF, 25 mL) at ambient temperature, and the reaction was stirred for 2 h. The reaction was acidified to pH 1 by the addition of dilute aqueous HCl, and the reaction was extracted with EtOAc (2  $\times$  100 mL). The combined organic layers were dried over Na<sub>2</sub>SO<sub>4</sub> and reduced in vacuo. The residue was dissolved in methanol (50 mL), 5% palladium on carbon (100 mg) was added, and the reaction was stirred at ambient temperature under a hydrogen atmosphere at ambient pressure for 14 h. The reaction was filtered, and the solvent was removed in vacuo. The residue was purified by recrystallization from EtOAc to give (S)-3 (509 mg, 81%).

(R)-N $\alpha$ -(Undecanoyl)glutamine (**3**) was synthesized in a similar fashion from (R)-glutamine in 78% yield.

(S)-N $\alpha$ -(Undecanoyl)glutamic Acid-1-amide (**4**). (S)- $\gamma$ -Benzyl-glutamate (2 mmol) and Na<sub>2</sub>CO<sub>3</sub> (6 mmol) in water (50 mL) were added to a solution of undec-10-enoyl chloride (2 mmol) in THF (25 mL) at ambient temperature, and the reaction was stirred for 2 h. The reaction was acidified to pH 1 by the addition of dilute aqueous HCl, and the reaction was extracted with EtOAc (2  $\times$  100 mL). The combined organic layers were dried over Na<sub>2</sub>CO<sub>3</sub> and reduced in vacuo. The

residue was dissolved in THF (20 mL) along with *N*-hydroxy succinimide (230 mg, 2 mmol), and dicyclohexylcarbodiimide (412 mg, 2 mmol) was added. The reaction was stirred for 12 h, filtered, and then concentrated, and aqueous ammonia (2 mL) was added. The reaction was stirred for an additional 4 h, and then the solvent was removed in vacuo. The residue was partitioned between water (50 mL) and EtOAc (2 × 100 mL). The combined organic layers were dried over Na<sub>2</sub>SO<sub>4</sub> and reduced in vacuo. The residue was dissolved in methanol (50 mL), 5% palladium on carbon (100 mg) was added, and the reaction was stirred at ambient temperature under a hydrogen atmosphere at ambient pressure for 14 h. The reaction was filtered, and the solvent was removed in vacuo. The residue was purified by recrystallization from EtOAc to give (S)-**4** (396 mg, 63%).

**(R)-N $\alpha$ -(Undecanoyl)glutamic acid-1-amide (4)** was synthesized in a similar fashion from (*R*)- $\gamma$ -benzyl-glutamate in 56% yield.

**(S)-N-(Undecanoyl)glutamic Acid (5).** (*S*)-Glutamic acid (2 mmol) and Na<sub>2</sub>CO<sub>3</sub> (8 mmol) in water (50 mL) were added to a solution of undec-10-enoyl chloride (2 mmol) in THF (25 mL) at ambient temperature, and the reaction was stirred for 2 h. The reaction was acidified to pH 1 by the addition of dilute aqueous HCl, and the reaction was extracted with EtOAc (2 × 100 mL). The combined organic layers were dried over Na<sub>2</sub>SO<sub>4</sub> and reduced in vacuo. The residue was dissolved in methanol (50 mL), 5% palladium on carbon (100 mg) was added, and the reaction was stirred at ambient temperature under a hydrogen atmosphere at ambient pressure for 14 h. The reaction was filtered, and the solvent was removed in vacuo. The residue was purified by recrystallization from EtOAc to give (S)-**5** (529 mg, 84%).

**(R)-N-(Undecanoyl)glutamic acid (5)** was synthesized in a similar fashion from (*R*)-glutamic acid in 91% yield.

**(S)-3-(10'-Undecenoylamino)-pyrrolidin-2-one (8).** (*S*)-3-Amino-pyrrolidinone<sup>20</sup> (**18**, 2 mmol) and Na<sub>2</sub>CO<sub>3</sub> (4 mmol) in water (25 mL) were added to a solution of undec-10-enoyl chloride (2 mmol) in dichloromethane (25 mL) at ambient temperature, and the reaction was stirred for 2 h. The organic layer was then separated, and the aqueous phase was extracted with additional dichloromethane (2 × 25 mL). The combined organic layers were dried over Na<sub>2</sub>CO<sub>3</sub> and reduced in vacuo. The residue was purified by recrystallization from EtOAc to give (S)-**8** (446 mg, 84%).

**(S)-3-(Undec-10'-enoyl)amino-azepan-2-one (9).** (*S*)-3-Amino-caprolactam hydrochloride (**19**, 2 mmol) and Na<sub>2</sub>CO<sub>3</sub> (6 mmol) in water (25 mL) were added to a solution of undec-10-enoyl chloride (2 mmol) in dichloromethane (25 mL) at ambient temperature, and the reaction was stirred for 2 h. The organic layer was then separated, and the aqueous phase was extracted with additional dichloromethane (2 × 25 mL). The combined organic layers were dried over Na<sub>2</sub>CO<sub>3</sub> and reduced in vacuo. The residue was purified by recrystallization from EtOAc to give (S)-**9** (423 mg, 72%).

**(S)-3-Undecanoylamino-azepan-2-one (10).** (*S*)-3-Amino-caprolactam hydrochloride (**19**, 2 mmol) and Na<sub>2</sub>CO<sub>3</sub> (6 mmol) in water (25 mL) were added to a solution of undecanoyl chloride (2 mmol) in dichloromethane (25 mL) at ambient temperature, and the reaction was stirred for 2 h. The organic layer was then separated, and the aqueous phase was extracted with additional dichloromethane (2 × 25 mL). The combined organic layers were dried over Na<sub>2</sub>CO<sub>3</sub> and reduced in vacuo. The residue was purified by recrystallization from EtOAc to give (S)-**10** (397 mg, 67%).

**(S)-3-(Undec-10'-ynoyl)amino-azepan-2-one (11).** (*S*)-3-Amino-caprolactam hydrochloride (**19**, 2 mmol) and Na<sub>2</sub>CO<sub>3</sub> (6 mmol) in water (25 mL) were added to a solution of undec-10-ynoyl chloride (2 mmol) in dichloromethane (25 mL) at ambient temperature, and the reaction was stirred for 2 h. The organic layer was then separated, and the aqueous phase was extracted with additional dichloromethane (2 × 25 mL). The combined organic layers were dried over Na<sub>2</sub>CO<sub>3</sub> and reduced in vacuo. The residue was purified by recrystallization from EtOAc to give (S)-**11** (362 mg, 62%).

**(S)-3-Dodecanoylamino-azepan-2-one (12).** (*S*)-3-Amino-caprolactam hydrochloride (**19**, 2 mmol) and Na<sub>2</sub>CO<sub>3</sub> (6 mmol) in water (25 mL) were added to a solution of dodecanoyl chloride (2 mmol) in dichloromethane (25 mL) at ambient temperature, and the reaction was stirred for 2 h. The organic layer was then separated, and the aqueous phase was extracted with additional dichloromethane (2 × 25 mL). The combined organic layers were dried over Na<sub>2</sub>CO<sub>3</sub> and reduced in vacuo. The residue was purified by recrystallization from EtOAc to give (S)-**12** (439 mg, 71%).

**(S)-3-Tetradecanoylamino-azepan-2-one (13).** (*S*)-3-Amino-caprolactam hydrochloride (**19**, 2 mmol) and Na<sub>2</sub>CO<sub>3</sub> (6 mmol) in water (25 mL) were added to a solution of tetradecanoyl chloride (2 mmol) in dichloromethane (25 mL) at ambient temperature, and the reaction was stirred for 2 h. The organic layer was then separated, and the aqueous phase was extracted with additional dichloromethane (2 × 25 mL). The combined organic layers were dried over Na<sub>2</sub>CO<sub>3</sub> and reduced in vacuo. The residue was purified by recrystallization from EtOAc to give (S)-**13** (412 mg, 61%).

**(S)-3-Hexadecanoylamino-azepan-2-one (14).** (*S*)-3-Amino-caprolactam hydrochloride (**19**, 5 mmol) and Na<sub>2</sub>CO<sub>3</sub> (15 mmol) in water (25 mL) were added to a solution of hexadecanoyl chloride (5 mmol) in dichloromethane (25 mL) at ambient temperature, and the reaction was stirred for 2 h. The organic layer was then separated, and the aqueous phase was extracted with additional dichloromethane (2 × 25 mL). The combined organic layers were dried over Na<sub>2</sub>CO<sub>3</sub> and reduced in vacuo. The residue was purified by recrystallization from EtOAc to give (S)-**14** (1.41 g, 77%).

**(R)-3-Hexadecanoylamino-azepan-2-one (14).** (*R,R*)-3-Amino-caprolactam hydro-pyrrolidine-5-carboxylate (**20**, 5 mmol) and Na<sub>2</sub>CO<sub>3</sub> (15 mmol) in water (25 mL) were added to a solution of hexadecanoyl chloride (5 mmol) in dichloromethane (25 mL) at ambient temperature, and the reaction was stirred for 2 h. The organic layer was then separated, and the aqueous phase was extracted with additional dichloromethane (2 × 25 mL). The combined organic layers were dried over Na<sub>2</sub>CO<sub>3</sub> and reduced in vacuo. The residue was purified by recrystallization from EtOAc to give (R)-**14** (1.23 g, 67%).

**(S)-3-Octadecanoylamino-azepan-2-one (15).** (*S*)-3-Amino-caprolactam hydrochloride (**19**, 2 mmol) and Na<sub>2</sub>CO<sub>3</sub> (6 mmol) in water (25 mL) were added to a solution of octadecanoyl chloride (2 mmol) in dichloromethane (25 mL) at ambient temperature, and the reaction was stirred for 2 h. The organic layer was then separated, and the aqueous phase was extracted with additional dichloromethane (2 × 25 mL). The combined organic layers were dried over Na<sub>2</sub>CO<sub>3</sub> and reduced in vacuo. The residue was purified by recrystallization from EtOAc to give (S)-**15** (648 mg, 82%).

**(S)-(Z)-3-(Hexadec-9'-enoyl)amino-azepan-2-one (16).** (*S,S*)-3-Amino-caprolactam hydro-pyrrolidine-5-carboxylate (**20**, 2 mmol) and Na<sub>2</sub>CO<sub>3</sub> (6 mmol) in water (25 mL) were added to a solution of (*Z*)-hexadec-9-enoyl chloride (2 mmol) in dichloromethane (25 mL) at ambient temperature, and the reaction was stirred for 2 h. The organic layer was then separated, and the aqueous phase was extracted with additional dichloromethane (2 × 25 mL). The combined organic layers were dried over Na<sub>2</sub>CO<sub>3</sub> and reduced in vacuo. The residue was purified by silica column chromatography (EtOAc to 9:1 EtOAc/MeOH) to give (S)-**16** (406 mg, 56%).

**(S)-(Z)-3-(Octadec-9'-enoyl)amino-azepan-2-one (17).** (*S,S*)-3-Amino-caprolactam hydro-pyrrolidine-5-carboxylate (**20**, 2 mmol) and Na<sub>2</sub>CO<sub>3</sub> (6 mmol) in water (25 mL) were added to a solution of (*Z*)-octadec-9-enoyl chloride (2 mmol) in dichloromethane (25 mL) at ambient temperature, and the reaction was stirred for 2 h. The organic layer was then separated, and the aqueous phase was extracted with additional dichloromethane (2 × 25 mL). The combined organic layers were dried over Na<sub>2</sub>CO<sub>3</sub> and reduced in vacuo. The residue was purified by silica column chromatography (EtOAc to 9:1 EtOAc/MeOH) to give (S)-**17** (514 mg, 66%).

**(R)-(Z)-3-(Octadec-9'-enoyl)amino-azepan-2-one (17).** (*R,R*)-3-Amino-caprolactam hydro-pyrrolidine-5-carboxylate (**20**,

2 mmol) and Na<sub>2</sub>CO<sub>3</sub> (6 mmol) in water (25 mL) were added to a solution of (*Z*)-octadec-9-enoyl chloride (2 mmol) in dichloromethane (25 mL) at ambient temperature, and the reaction was stirred for 2 h. The organic layer was then separated, and the aqueous phase was extracted with additional dichloromethane (2 × 25 mL). The combined organic layers were dried over Na<sub>2</sub>CO<sub>3</sub> and reduced in vacuo. The residue was purified by silica column chromatography (EtOAc to 9:1 EtOAc/MeOH) to give (*R*)-**17** (574 mg, 73%).

**Biological Assays.** Compounds were tested for their ability to inhibit chemokine-induced migration using the microtiter format trans-well migration assay, exactly as described previously.<sup>12,17,23</sup> All migration assays were performed in Gey's balanced salt solution containing 1 mg/ml endotoxin-free BSA (in the absence of fetal calf serum), allowing migration to occur for 2 h at 37 °C. All compounds were solubilized in DMSO and added to both the top and the bottom compartments of the trans-well migration plate at a constant final DMSO concentration of 1%.

The effect of target compounds on TNF-α upregulation in vivo was determined exactly as previously,<sup>17</sup> except that the vehicle used was 0.6% DMSO and 1% carboxymethylcellulose (final concentrations) in sterile water. Values reported as the mean ± standard error for each group (*n* = 6).

**Supporting Information Available:** Characterization data for compounds **3–5** and **8–17**, HPLC conditions, and statistical analysis of biological data. This material is available free of charge via the Internet at <http://pubs.acs.org>.

## References

- (1) Bebo, B. F., Jr.; Yong, T.; Orr, E. L.; Linthicum, D. S. Hypothesis: A possible role for mast cells and their inflammatory mediators in the pathogenesis of autoimmune encephalomyelitis. *J. Neurosci. Res.* **1996**, *45*, 340–348.
- (2) Franceschi, C.; Bonafe, M.; Valensin, S.; Olivieri, F.; De Luca, M.; Ottaviani, E.; De Benedictis, G. Inflamm-aging—An evolutionary perspective on immunosenescence. *Ann. NY Acad. Sci.* **2000**, *908*, 244–254.
- (3) Mennicken, F.; Maki, R.; de Souza, E. B.; Quirion, R. Chemokines and chemokine receptors in the CNS: A possible role in neuroinflammation and patterning. *Trends Pharmacol. Sci.* **1999**, *20*, 73–78.
- (4) Rogers J.; Shen, Y. A perspective on inflammation in Alzheimer's disease. *Ann. NY Acad. Sci.* **2000**, *924*, 132–135.
- (5) Sullivan, G. W.; Sarembock, I. J.; Linden, J. The role of inflammation in vascular diseases. *J. Leukocyte Biol.* **2000**, *67*, 591–602.
- (6) Watanabe T.; Fan, J. L. Atherosclerosis and inflammation—Mononuclear cell recruitment and adhesion molecules with reference to the implication of ICAM-1/LFA-1 pathway in atherogenesis. *Int. J. Cardiol.* **1998**, *66* (Suppl 1), S45–S53.
- (7) Gerard, C.; Rollins, B. J. Chemokines and disease. *Nat. Immunol.* **2001**, *2*, 108–115.
- (8) Horuk, R. Chemokine receptors. *Cytokine Growth Factor Rev.* **2001**, *12*, 313–335.
- (9) Rollins, B. J.; Chemokines. *Blood* **1997**, *90*, 909–928.
- (10) Luster, A. D. Chemokines—Chemotactic cytokines that mediate inflammation. *N. Engl. J. Med.* **1998**, *338*, 436–445.
- (11) Thelen, M. Dancing to the tune of chemokines. *Nat. Immunol.* **2001**, *2*, 129–134.
- (12) Reckless, J.; Grainger, D. J. Identification of oligopeptide sequences which inhibit migration induced by a wide range of chemokines. *Biochem. J.* **1999**, *340*, 803–811.
- (13) Reckless, J.; Tatalick, L. M.; Grainger, D. J. The pan-chemokine inhibitor NR58–3.14.3 abolishes tumour necrosis factor-α accumulation and leucocyte recruitment induced by lipopolysaccharide in vivo. *Immunology* **2001**, *103*, 244–254.
- (14) Grainger D. J.; Reckless, J. Broad-spectrum chemokine inhibitors (BSCIs) and their anti-inflammatory effects in vivo. *Biochem. Pharmacol.* **2003**, *65*, 1027–1034.
- (15) Naidu, B. V.; Farivar, A. S.; Krishnadasan, B.; Woolley, S. M.; Grainger, D. J.; Verrier, E. D.; Mulligan, M. S. Broad-spectrum chemokine inhibition ameliorates experimental obliterative bronchiolitis. *Ann. Thorac. Surg.* **2003**, *75*, 1118–1122.
- (16) Wilbert, S. M.; Engrissei, G.; Yau, E. K.; Grainger, D. J.; Tatalick, L.; Axworthy, D. B. Quantitative analysis of a synthetic peptide, NR58-3.14.3, in serum by LC-MS with inclusion of a diastereomer as internal standard. *Anal. Biochem.* **2000**, *278*, 14–21.
- (17) Fox, D. J.; Reckless, J.; Warren, S. G.; Grainger, D. J. Design, synthesis, and preliminary pharmacological evaluation of *N*-acyl-3-aminoglutarimides as broad-spectrum chemokine inhibitors in vitro and anti-inflammatory agents in vivo. *J. Med. Chem.* **2002**, *45*, 360–370.
- (18) Reist, M.; Carrupt, P. A.; Francotte, E.; Testa, B. Chiral inversion and hydrolysis of thalidomide: Mechanisms and catalysis by bases and serum albumin, and chiral stability of teratogenic metabolites. *Chem. Res. Toxicol.* **1998**, *11*, 1521–1528.
- (19) Eriksson, T.; Bjorkman, S.; Roth, B.; Fyge, A.; Hoglund, P. Enantiomers of thalidomide: Blood distribution and the influence of serum albumin on chiral inversion and hydrolysis. *Chirality* **1998**, *10*, 223–228.
- (20) Pellegata, R.; Pinza, M.; Pifferi, G. An improved synthesis of gamma-, delta-, and epsilon-lactams. *Synthesis* **1978**, 614–616.
- (21) Rezler, E. M.; Fenton, R. R.; Esdale, W. J.; McKeage, M. J.; Russell, P. J.; Hambley, T. W. Preparation, characterization, DNA binding, and in vitro cytotoxicity of the enantiomers of the platinum(II) complexes *N*-methyl-, *N*-ethyl- and *N,N*-dimethyl-(*R*-) and -(*S*-)-3-aminohexahydroazepinedichloroplatinum (II). *J. Med. Chem.* **1997**, *40*, 3508–3515.
- (22) Boyle, W. J.; Sifniades, S.; Van Peppen, J. V. Asymmetric transformation of α-amino-ε-caprolactam, a lysine precursor. *J. Org. Chem.* **1979**, *44*, 4841–4847.
- (23) Frow, E. K.; Reckless J.; Grainger, D. J. Tools for anti-inflammatory drug design: In vitro models of leukocyte migration. *Med. Res. Rev.* **2004**, *24*, 276–298.

JM049365A